Charging of Au Atoms on TiO_2 Thin Films from CO Vibrational Spectroscopy and DFT Calculations

Anke S. Wörz and Ueli Heiz

Lehrstuhl für Physikalische Chemie 1, Technische Universität München, D-85747 Garching, Germany

Fabrizio Cinquini and Gianfranco Pacchioni*

Dipartimento di Scienza dei Materiali, Università di Milano-Bicocca, Via R. Cozzi, 53-20125, Milano, Italy

Received: July 25, 2005

Au atoms have been deposited on oxidized and reduced TiO_2 thin films grown on Mo(110). The gold binding sites and the occurrence of Au−TiO_2 charge transfer were identified by measuring infrared spectra as a function of temperature and substrate preparation. The results have been interpreted by slab model DFT calculations. Au binds weakly to regular TiO_2 sites (D_e < 0.5 eV) where it remains neutral, and diffuses easily even at low temperature until it gets trapped at strong binding sites such as oxygen vacancies (D_e = 1.7 eV). Here, a charge transfer from TiO_2 to Au occurs. $Au^{\delta-}CO$ complexes formed on oxygen vacancies easily lose CO (D_e = 0.4 eV), and the CO stretching frequency is red-shifted. On nondefective surfaces, CO adsorption induces a charge transfer from Au to TiO_2 with formation of strongly bound $Au^{\delta+}CO$ complexes (D_e = 2.4 eV); the corresponding CO frequency is blue-shifted with respect to free CO. We propose possible mechanisms to reconcile the observed CO desorption around 380 K with the unusually high stability of Au−CO complexes formed on regular sites predicted by the calculations. This implies: (a) diffusion of AuCO complexes above 150 K; (b) formation of gold dimers when the diffusing AuCO complex encounters a Au atom bound to an oxygen vacancy (reduced TiO_2) or a second AuCO unit (oxidized TiO_2); and (c) CO desorption from the resulting dimer, occurring around 350−400 K.

Introduction

The adsorption of Au atoms, clusters, and particles on TiO_2 surfaces is without any doubt the most intensively studied problem in the field of supported metal clusters on oxides under controlled conditions.[1−21] This intense activity is stimulated by the not yet resolved problem of the catalytic activity in CO oxidation promoted by small Au particles deposited on titania discovered by Haruta some years ago.[22] Since then, a particularly intense experimental and theoretical effort was made to clarify the mechanism of the interaction and the reasons for the special activity of supported gold nanoparticles. The interest stems from the fact that Au has been known to be a rather inert species, so that several questions arose from the Haruta discovery. A number of important observations have been done, although the firm points are probably still less numerous than the open questions. These are related to the role of the substrate, that of surface defects (in particular oxygen vacancies), the effect of particle size and shape, the occurrence of strong metal support interaction (SMSI), etc. With regards to the mechanism of CO oxidation on the Au_n/TiO_2 surface, while some authors have suggested that the reaction involves atomic oxygen produced by the easy dissociation of O_2, most authors believe that the oxidizing species is molecular oxygen because the barrier for O_2 dissociation is quite high. Furthermore, there is a strong particle size dependence of the reactivity; see ref 23 and references therein.

In a number of recent experiments, it has been shown that the activity of Au nanoclusters can be considerably increased by charging the cluster negative. Even a gas-phase Au_2 molecule can catalyze the conversion of CO to CO_2, provided that the species carries an extra charge.[24] Recent experiments on Au clusters deposited on MgO have shown the crucial role of oxygen vacancies in increasing the electron density on the cluster and hence its reactivity.[25,26] These studies have demonstrated the very important role that defects on oxide surfaces play in modifying the activity of a supported metal cluster. This is true even for isolated atoms: Pd atoms deposited on defect-rich MgO surfaces are active in promoting the cyclotrimerization of acetylene to benzene, at variance with the same atoms sitting on regular sites of the surface.[27] However, the consensus on the role of charging is not unanimous: from XPS and chemical activity results, Arrii et al.[21] concluded that the existence of negatively charged particles is not the key point to explain the high activity observed for Au/TiO_2 and Au/ZrO_2 catalysts but that this is related to the direct participation of titania and zirconia substrates in the catalytic process. For this reason, a detailed understanding of the chemical reactivity of a supported cluster/particle requires a careful investigation of both the nature of the cluster-substrate interaction and the site where the nucleation or stabilization of the cluster has occurred. Recently, we have shown how the combined use of infrared (IR) spectroscopy, thermal desorption spectroscopy, and DFT calculations on CO adsorbed on Pd atoms deposited on MgO thin films can provide detailed information about the sites where the metal atoms are stabilized as well as on the nature of the metal−oxide interaction, including the occurrence of charge transfers at the interface.[28]

In this paper, we propose a similar scheme where mass-selected Au atoms have been deposited on reduced and oxidized

* Corresponding author. E-mail: gianfranco.pacchioni@unimib.it.

10.1021/jp054093o CCC: $30.25
Published on Web 09/08/2005

TiO_2 thin films grown on Mo(110). CO has been used as a source of information on the interaction of the Au atoms with the substrate. The experimental results have been interpreted on the basis of plane wave supercell DFT calculations. The scope of the paper is to identify the sites where the Au atoms are bound preferentially, their diffusion mechanisms before and after exposure to CO, and, most important, the occurrence of charge transfers between the TiO_2 surface and gold. Here, we provide unambiguous evidence of the occurrence of charge transfer from TiO_2 vacancies to Au, and we show that the adsorption of CO on Au atoms sitting on regular bridging oxygen sites results in the opposite effect, that is, charge transfer from Au to the TiO_2 substrate. This leads to complex diffusion paths as the temperature is increased and finally results in the desorption of CO molecules from Au dimers. It is not the first time that it is suggested that Au atoms or clusters bound to various sites of the TiO_2 surface give rise to charge transfers from or to the oxide. Some theoretical studies have predicted the occurrence of charge transfer from oxygen vacancies to adsorbed Au atoms[9,10,19] (but others concluded that Au is neutral).[12] Boccuzzi et al.[16] found that on reduced TiO_2 surfaces CO bound to Au nanoclusters result in substantial red-shifts in IR frequencies attributed to the negative charge associated with surface vacancies. A similar conclusion was reached by Lee et al. based on XPS results on Au_1/TiO_2.[20] The novelty of this study consists of the study of Au−CO complexes formed on reduced and oxidized TiO_2 films, in the measurement of their vibrations and thermal stability, and in the interpretation of the results based on atomistic models derived from first principles DFT calculations. Particularly, we show that depending on the trapping center gold atoms can be charged differently on TiO_2 and consequently that the population of the trapping centers and the diffusion behavior of gold are primordial for the catalytic activity. From the combined use of these complementary approaches, a unified picture of the $CO/Au_1/TiO_2$ system as a function of temperature is presented.

The paper is organized as follows. After a brief description of the experimental and theoretical details, we report the experimental results where the IR spectra are described, and the results of the DFT calculations for Au_1 and CO adsorption. The two sets of results are then compared and discussed. Conclusions are summarized in the last section.

Experimental Details

For the experimental study of the interaction between gold atoms and TiO_2, thin films were prepared in situ. CO was used as a probe molecule to estimate charge transfers between the Au atoms and the support by means of IR spectroscopy. The value of the CO stretch frequencies is a good indicator of the charge of Au_1 because it is changing with the degree of donation and back-donation between CO and Au_1 and thus reflects the charge transfer between the gold atom and the support.

According to the preparation method described by Goodman and co-workers,[29−31] thin TiO_2 films are epitaxially grown by evaporating Ti in an O_2 background onto a Mo(110) single crystal. The physical and chemical properties of such thin films have been studied in detail by this group. They found a strong dependence between the preparation conditions and the morphology and chemical composition by varying the oxygen pressure or annealing temperature. Films growing at a substrate temperature between 600 and 700 K in an O_2 background of 2×10^{-7} mbar, followed by annealing with O_2 (10^{-7} mbar) and without O_2 at 800 K, are most probable stoichiometric $TiO_2(100)$ films with rutile structure.[30]

The TiO_2 thin films used in our experiments are produced in situ before each experiment by evaporating the Ti with an evaporation rate of 0.8 ML/min in O_2 (5×10^{-7} mbar) onto a Mo(110) single crystal, followed by annealing to 670 K in O_2 (5×10^{-7} mbar). During the film growth, the Mo(110) substrate was kept at 620 K. With this procedure, oxidized films are obtained. To obtain reduced films, the sample was further annealed to 950 K. For the experiments, we used films with thicknesses between 7 and 10 monolayers (ML, 1 ML = 2.25×10^{15} atoms/cm^2). We expect that the surface morphology of the reduced and oxidized films is the same since Lai et al.[31] described the surface morphology to change from a flat, smooth surface to a rough surface with 3D crystallites if they are annealed to higher temperatures (∼1200 K). We also assume to get reduced films by annealing the sample without oxygen and to get oxidized films by exposing them to oxygen during annealing. It is well known from single-crystal studies that oxygen vacancies are created by thermal treatment and removed if the samples are annealed in oxygen.[32−37]

The gold atom cations are generated by laser ablation and are subsequently mass separated by radio frequency electric quadrupole fields.[38] The ions are then deposited with low kinetic energy onto thin, in situ grown TiO_2 films and are neutralized upon deposition by electron tunneling through the films. For the experiments, we deposited 1% ML of gold atoms. The gas-phase separation of the atoms from other aggregates in the molecular beam, the low temperature at which the substrate is kept during deposition (90 K), and the low concentration of adsorbates are all elements that guarantee that isolated atoms and not clusters or particles are present on the surface. These can form only upon diffusion of the monomeric species as the temperature is increased, as discussed to some extent below.

Experiments were performed in two different ways: (1) gold atoms are deposited onto the TiO_2 thin film in a ^{13}CO background of 1×10^{-8} mbar; and (2) ^{13}CO (0.45 Langmuir, 1 L = 1×10^{-6} Torr s) was dosed after gold atoms deposition. In both cases, infrared spectra are taken at various temperatures. Both types of infrared experiments were done on oxidized as well as on reduced TiO_2 films.

Computational Details

The calculations are based on density functional theory (DFT) at the level of the generalized gradient approximation (using the PW-91 exchange-correlation functional).[39] The method is implemented in the VASP program,[40,41] which uses a plane wave basis set (with a kinetic energy cutoff at 396 eV) and ultrasoft pseudopotentials[42] for the electron−ion interactions. The atoms within the supercell are relaxed until the atomic forces are less than 0.02 eV/Å. Within this approach, the optimized bulk lattice parameters of rutile TiO_2 are a = 4.658 Å, c = 2.977 Å, u = 0.305. For the $TiO_2(110)$ slabs, we used a $c(4 \times 2)$ unit cell corresponding to a coverage $\theta = 0.125$ (following Onishi et al.'s definition,[43] $\theta = 0.125$ monolayer corresponds to a metal atom adsorbed for each four Ti_{5c} atoms). The calculations have been done at the Γ point. The slabs were separated by at least 10 Å of vacuum. The positions of all atoms of the supercell except those in the bottom layer were optimized by means of a conjugate gradient optimization algorithm. For the electronic structure calculations, a Gaussian broadening of the electronic levels with $\delta = 0.2$ eV was applied.

Convergence of adsorption properties with the thickness of the TiO_2 slab is a serious problem that has been discussed in the literature in some detail.[8,10,44−46] Recently, we have shown that the energy gap (E_g) of a TiO_2 rutile film changes with the

TABLE 1: Dependence of Bond Strengths (in eV) for TiO_2AuCO on Number of Layers (nL) and Geometrical Relaxation in the Film

	Au site[a]	4L (1;3)[b]	5L (1;4)[b]	5L (2;3)[b]
TiO_2-Au_1	OT	0.36	0.55	0.66
	OV	1.73	1.86	1.57
TiO_2Au_1-CO	OT	2.42	2.53	2.51
	OV	0.41	0.36	0.38
$TiO_2-Au1CO$	OT	2.05	2.37	2.45
	OV	1.42	1.15	1.24

[a] OT = on-top of O_{2c}; OV = oxygen vacancy, missing O_{2c} atom. See also Figure 3. [b] In parentheses, the number of fixed and free layers, respectively, in the geometry optimization.

number of layers (nL) in the film and that strong odd−even oscillations occur depending on the presence of a symmetry plane in the slab.[47] These oscillations reflect the changes in interlayer distances, and in particular in the distance of the second layer from the third one. Only after 10 TiO_2 layers (30 atomic layers) does E_g converge to the bulk value.[47] Clearly, a 10L film is too big for present possibilities to simulate the rutile surface, and thinner slabs must be used. In a recent study on water adsorption, the use of an empirical correction to the results obtained with a 3L and a 4L slab has been suggested.[48] Here, we have checked the results by using 4L and 5L TiO_2 slabs, keeping fixed the bulk positions the atoms in the bottom layer or in the two bottom layers, respectively. The results, Table 1, show that there are oscillations in the TiO_2-Au_1, TiO_2Au_1-CO , or TiO_2-Au_1CO bond strengths up to 0.3 eV. While this is not too severe when the binding energy is large (e.g., that of CO to Au bound on bridging oxygens, >2 eV), the oscillation is quite strong when one deals with the binding of Au with the surface (<1 eV). On the other hand, the geometries of the adsorbed species are practically the same for different substrate thickness. Therefore, one has to be aware of the fact that the computed adsorption energies have only a semiquantitative value and should not be taken literally. Despite this limitation, the analysis of the results and of the general features of TiO_2AuCO is sufficient to draw some general firm conclusions about the properties of this system. For the calculations, we decided to use a 4L slab where the atoms of the bottom layer are fixed at the bulk positions.

Experimental Results

Here, we present the results of an infrared study performed in two different ways: in a first type of experiments, we deposited the gold atoms in a ^{13}CO background of 1×10^{-8} mbar, and in a second type, the ^{13}CO (0.3 L) was dosed after the gold atoms are deposited under UHV conditions.

The results of these measurements on oxidized films are depicted in Figure 1. Figure 1a−g shows IR absorption bands if Au_1 is deposited in a ^{13}CO atmosphere. There are two main bands at 120 K, one at 2141 cm^{-1} and another at 2124 cm^{-1} (Figure 1a). At a temperature of 175 K, only the band at 2123 cm^{-1} is still clearly visible with a small shoulder at 2143 cm^{-1}, reminiscent from the band at 2141 cm^{-1} observed at 120 K. The intensity of the remaining IR absorption band is stable up to 275 K and disappears between 330 and 380 K (Figure 1b−g). If ^{13}CO was dosed after gold atom deposition, only a very small band at 2139 cm^{-1} (Figure 1h) is apparent, which disappears at a temperature of 175 K (spectra not shown here). In summary, these results reveal a single strong ^{13}CO absorption band if Au_1 are deposited in a ^{13}CO background, and they show that this absorption is apparent up to temperatures between 330 and 380 K.

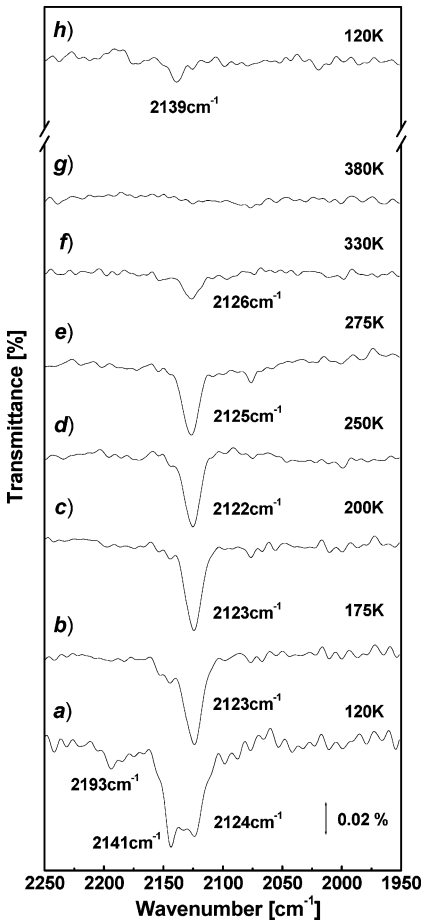

Figure 1. Shown are the infrared spectra measured after Au_1 was deposited in an ^{13}CO background of 1×10^{-8} mbar onto oxidized TiO_2 thin films (Figure 1a−g) as well as the spectra when the gold atoms are deposited onto the oxidized TiO_2 thin films and ^{13}CO (0.3 L) was dosed after deposition (Figure 1h). In both cases, an amount of 1.0% ML of gold atoms are deposited.

The same experiments are repeated with reduced TiO_2 films (Figure 2). The spectra in Figure 2a−f show the results if the gold atoms are deposited in ^{13}CO. At 120 K, there is one main band at 2136 cm^{-1} with a small shoulder at 2123 cm^{-1} and two weak bands at 2178 and 2083 cm^{-1}. While the main band decreases drastically when annealed to 175 K, the shoulder at ∼2126 cm^{-1} evolves into a distinct absorption band. This band is apparent up to temperatures around 330 K. If ^{13}CO is dosed after the deposition, there is only a main band at 2136 cm^{-1} observed with two weaker contributions at 2178 and 2083 cm^{-1}, Figure 2. All bands are absent already at 175 K. From all of these data of the oxidized and reduced films, it becomes clear that the band at 2123 cm^{-1} is absent if ^{13}CO is dosed after the deposition, while this absorption is apparent up to 330 K if the gold atoms are deposited in ^{13}CO.

The band around 2140 cm^{-1} can be assigned to ^{13}CO adsorbed on the TiO_2 thin films as it is also apparent if ^{13}CO was dosed on a plain film (results not shown here). Considering an isotope shift of 50 cm^{-1} going from ^{13}CO to ^{12}CO, this would correspond to a band at around 2190 cm^{-1}, close to that observed experimentally for CO adsorbed on five-coordinated Ti ions on the TiO_2 rutile surfaces.[55,56] Of course, we cannot exclude that CO also binds to low-coordinated ions of the TiO_2 films present at step edges. Nevertheless, on plain TiO_2 only one CO absorption was detected, indicating that CO is only adsorbed on one adsorption site. If we now compare the results for oxidized and reduced films, it becomes clear that there is

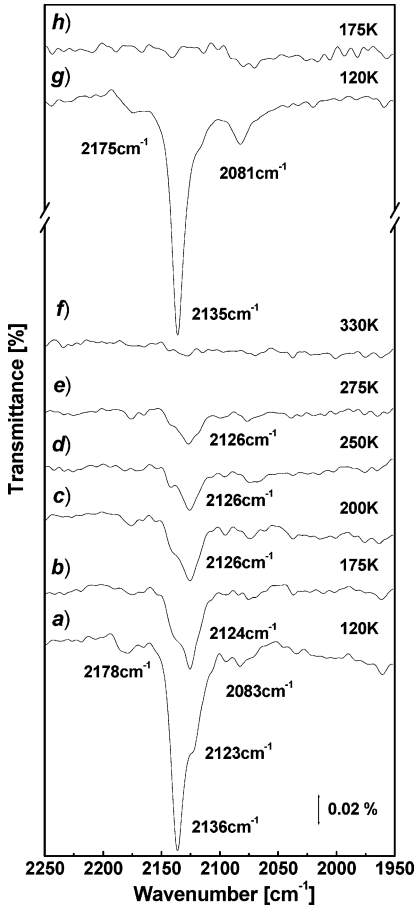

Figure 2. Shown are the infrared spectra measured after Au_1 was deposited in an ^{13}CO background of 1×10^{-8} mbar onto reduced TiO_2 thin films (Figure 2a−f) as well as the spectra when the gold atoms are deposited onto the oxidized TiO_2 thin films and ^{13}CO (0.3 L) was dosed subsequently (Figure 2g,h). In both cases, an amount of 1.0% ML of gold atoms are deposited.

only one distinct ^{13}CO absorption band for reduced films but not for oxidized films if ^{13}CO was dosed subsequently. The spectra measured if the gold atoms are deposited in ^{13}CO atmosphere show differences, too. While both bands at 2140 and 2123 cm^{-1} are of equal intensity at 120 K, on oxidized films the first one is visible as a small shoulder for reduced films. By increasing the temperature by a few kelvin, however, this shoulder becomes dominant. There are no stretch frequencies above 330 K on reduced films, while the one at 2126 cm^{-1} disappears between 330 and 380 K on oxidized films.

Considering all of these results, we conclude that the band around 2125 cm^{-1} is related to ^{13}CO adsorbed on gold atoms located on terrace sites and that these species are quite stable up to temperatures higher than 300 K. The band at 2083 cm^{-1} may be related to ^{13}CO adsorbed on Au_1 located on defect sites. This ^{13}CO/Au complex is not very stable because the band already disappears below 200 K.

Computational Results

Au Atoms on TiO_2. A gold atom has been adsorbed on various sites of the TiO_2(110) rutile surface: on-top of Ti_{5c} (T), on-top of a bridging oxygen O_{2c} (OT), in a bridge position over two bridging oxygens (OB), or on a three-hollow site formed by two basal and one bridging oxygen (OH); see Figure 3. In all cases, the bonding is weak, going from 0.55 eV (OH) to 0.21 eV (OB), Table 2. This is in general agreement with other studies of gold atoms on rutile or anatase surfaces,[5,8−10,18] while

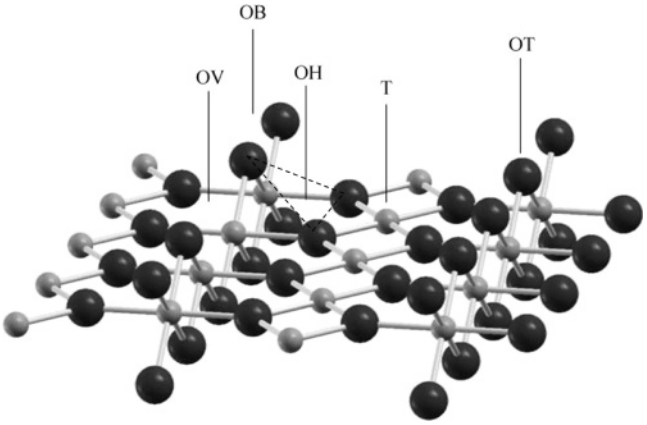

Figure 3. Schematic representation of adsorption sites on the TiO_2(110) rutile surface. OT = on-top of O_{2c}; OB = bridge position over two O_{2c} atoms; OH = hollow position over two O_{3c} and one O_{2c} atom; T = on-top of Ti; OV = oxygen vacancy, missing O_{2c} atom.

TABLE 2: Binding Energies, D_e in eV, of Au Atoms and AuCO Complexes on TiO_2 and of CO Adsorbed on TiO_2Au_1

site[a]	TiO_2-Au_1	TiO_2-Au_1CO	TiO_2Au_1-CO
OT	0.36	2.05	2.42
OB	0.21	1.72	2.23
OH	0.55	*b*	*b*
T	0.42	*b*	*b*
OV	1.73	1.42	0.41

[a] OT = on-top of O_{2c}; OB = bridge position over two O_{2c} atoms; OH = hollow position over two O_{3c} atoms and one O_{2c} atom; T = on-top of Ti; OV = oxygen vacancy, missing O_{2c} atom. See also Figure 3. [b] Unstable.

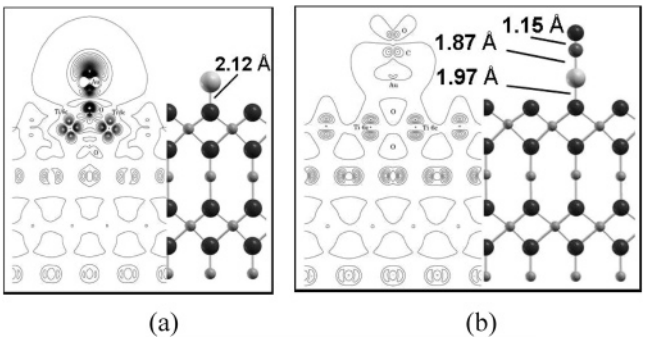

Figure 4. (a) Spin density plot and optimal geometry of a Au atom adsorbed on-top of a bridging oxygen (OT site); (b) spin density plot and optimal geometry of a AuCO complex formed on-top of a bridging oxygen (OT site).

it differs from the calculated bond strength of 1.55 eV reported by Wahlström et al.[12] Spin density maps (in Figure 4a reported for Au on a OT site) show that the Au adatom keeps the gas-phase electronic configuration, $5d^{10}6s^1$, with one electron occupying the 6s orbital. Thus, the isolated atom is practically neutral, and little or no charge transfer occurs between the adsorbate and the surface. The bonding arises from electron polarization effects, with small covalent contributions. The consequence is that Au atoms are able to diffuse almost freely on the surface. In fact, the computed barrier for diffusion along the bridging oxygen rows, about 0.15 eV, is so low that high mobility of the Au atoms is expected above liquid nitrogen temperature.

Things change dramatically on point defects such as the oxygen vacancies. Oxygen vacancies on TiO_2 are characterized by the presence of two reduced Ti^{3+} atoms near the vacancy; the electrons formally associated with the O^{2-} ion occupy the

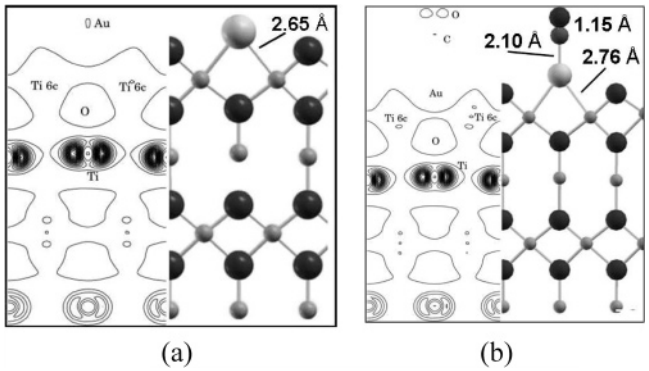

Figure 5. (a) Spin density plot and optimal geometry of a Au atom adsorbed on an oxygen vacancy (OV site); (b) spin density plot and optimal geometry of a AuCO complex formed on an oxygen vacancy (OV site).

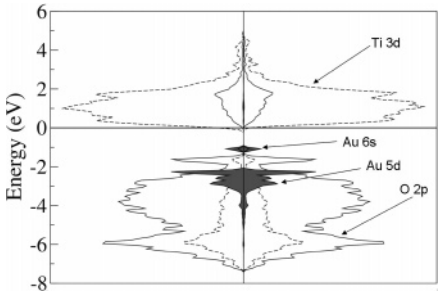

Figure 6. DOS curves for a Au atom adsorbed on-top of an oxygen vacancy. DOS of Au multiplied by 2. The DOS curves have been obtained by sampling of the Brillouin zone in a (4 × 4 × 1) k-points mesh.

localized 3d orbitals of two Ti atoms, which become spin polarized.[49] Therefore, the creation of oxygen vacancies on the surface of rutile is expected to result in two unpaired electrons associated with two subsurface Ti atoms. On oxygen vacancies, the Au atom is bound by 1.6−1.8 eV depending on the TiO_2 film thickness, with a binding energy 4 times larger than on the regular surface, Table 2. Similar or larger values have been reported by other authors.[8−10] Therefore, oxygen vacancies represent strong trapping sites where the diffusion process is blocked. The minimum energy required to detach a Au atom from a vacancy site is of the order of 1.3−1.4 eV, which suggests thermal stability for these species up to 500 K. When we consider the spin density plot of a Au atom bound to an oxygen vacancy, Figure 5a, we find that the spin is localized inside TiO_2 and that there is no spin density on the adsorbed Au atom. This can have only two origins: either the Au atom has transferred one electron to TiO_2, becoming Au^+, or it has taken charge from the substrate becoming Au^-. The second hypothesis is the correct one. It can be explained by the analysis of the density of states (DOS), which shows that the 6s level of Au is filled and falls below the Fermi level, Figure 6. Thus, the electronic configuration of a Au atom bound to an oxygen vacancy is formally $5d^{10}6s^2$. The formation of a negatively charged Au^- ion is not surprising if we consider that gold has a high electron affinity (EA) (2.31 eV according to both experiment[50] and calculations[51]). Charge transfer from an O vacancy on TiO_2 to adsorbed gold is somewhat controversial: some authors concluded that the Au-vacancy bond is covalent with no charge transfer,[12] while other theoretical studies based on the analysis of the electron distribution concluded in favor of the charge transfer.[9,10,19]

To summarize this section, we have found, in agreement with previous results, that Au atoms are weakly bound on regular sites of the rutile surface while they are strongly trapped at oxygen vacancies. Therefore, atoms arriving from the gas-phase have a high probability to diffuse on the surface even at low temperature, until they bind to a point defect (most likely an oxygen vacancy). In this case, an electron transfer occurs from TiO_2, with formation of Au^-.

CO Adsorbed on Au_1/TiO_2. A CO molecule has been adsorbed on the supported Au atoms to check the nature of the interaction between the metal and the TiO_2 substrate. We also tried to adsorb a second CO molecule on TiO_2Au_1; in fact, Pd and Rh atoms on MgO exposed to CO form $M(CO)_2$ and even $M(CO)_3$ supported complexes.[52] However, we found that the second CO molecule does not bind to AuCO formed on OT sites. The Au−CO complex is linear with r(Au−C) = 1.87 Å and r(C−O) = 1.150 Å, Figure 4b. The adsorption energy of CO on TiO_2Au_1 changes dramatically with the site where gold is bound. On the bridging oxygen rows (OT site), the Au−CO bond is very strong, 2.42 eV; on oxygen vacancies (OV site), the Au−CO bond is very weak, 0.41 eV, Table 2. In this second case, the bond strength is practically the same as for CO bound directly on-top on the Ti^{4+} five-coordinated cations (T site), 0.40 eV, a value almost coincident with the experimental one, 0.43 eV, measured for CO on TiO_2(110).[53] The Au−CO gas-phase complex is bound by 0.72 eV, that is, more than for Au−CO formed on a vacancy, but much less than for Au−CO formed on a bridging oxygen. The strong change in D_e going from the free to the supported AuCO complex, from 0.7 to 2.4 eV, clearly reflects a strong modification of the AuCO interaction induced by the substrate.

We consider first the AuCO complex formed on the non-defective TiO_2 surface (OT site, Figure 3). Here, gold is weakly adsorbed and no charge transfer occurs. However, when a CO molecule is added, a strong change in the metal−support interaction is observed: the 6s electron of Au is transferred to the Ti 3d states, Au becomes formally Au^+, and the TiO_2 substrate is reduced. The Pauli repulsion with the CO 5σ orbital destabilizes the 6s level of Au, which is pushed above the Fermi level; the 6s electron is transferred to the substrate, and there is almost no spin density left on gold, Figure 4b. In this way, the CO molecule can get closer to the Au atom where it forms a strong bond, 2.42 eV, Table 2; the bonding has a large σ donation contribution, involving the CO 5σ and the Au 6s orbitals. It is remarkable that the computed bond strength is very close to that measured experimentally for the gas-phase Au^+−CO complex, 2.08 ± 0.15 eV.[54] The occurrence of a Au → TiO_2 charge transfer is demonstrated, beside the spin density plot, Figure 4b, by the blue-shift in CO vibrational frequency (see below) typical of CO adsorbed on metal cations, and it has been suggested to occur also for AuCO complexes formed on the surface of anatase TiO_2.[19] It is also consistent with the shift to higher binding energies of the Au 4f levels measured in XPS experiments when CO is adsorbed on Au atoms dispersed on titania.[20]

A completely different situation is found when CO is bound to a Au atom stabilized at an oxygen vacancy. Here, the Au atom formally carries a negative charge, so that the Au 6s level is doubly occupied. The Pauli repulsion of the diffuse Au 6s and CO 5σ orbitals leads to a long equilibrium distance and a weak bonding. The Au−CO complex is bent forming an AuCO angle of 148°, with r(Au−C) = 2.10 Å and r(C−O) = 1.151 Å, Figure 5b. The $Au^{\delta-}$ anion is so stable when bound to the oxygen vacancy that the bonding with CO is not sufficient to destabilize the Au 6s level and induce a charge transfer toward the TiO_2 substrate, as was observed for gold sitting on regular

TABLE 3: Comparison of Measured and Computed Frequencies, ω_e in cm^{-1}, and Tentative Assignments for CO Adsorbed on Au_1/TiO_2

		exp.		theory[a]
system	adsorption site[b]	^{13}CO	^{12}CO	^{12}CO
CO		2093	2143	2143
AuCO				2097
TiO_2CO	T	~2140	~2190	2197
TiO_2Au_1CO	OT	~2125	~2175	2151
TiO_2Au_1CO	OV	~2080	~2129	2073

[a] Scaled frequencies (a scaling factor 2143/2104 = 1.0185 has been applied). [b] T = on-top of Ti; OT = on-top of O_{2c}; OV = oxygen vacancy, missing O_{2c} atom. See also Figure 3.

sites. Therefore, even in the presence of CO the anionic nature of the metal atom is preserved.

Thus, AuCO complexes formed on regular and defect sites have completely different electronic properties: while on regular sites they can be classified as Au^+-CO species, on the vacancy sites they formally correspond to Au^--CO. In reality, the real charge on the Au atom is not ± 1 as it is largely delocalized over the surface. Nevertheless, one should be able to discriminate between the two species by studying the vibrational properties of adsorbed CO. To this end, we have computed the vibrational frequencies of TiO_2Au_1CO complexes, Table 3. To take into account intrinsic errors in the DFT calculation of vibrational frequencies and anharmonic effects, a scaling factor is applied to all frequencies (see Table 3). Notice that our computed values refer to ^{12}CO, while the experimental data reported above are for ^{13}CO. An isotope shift of 50 cm^{-1} has been added to the ^{13}CO frequencies to compare them with those of ^{12}CO; see Table 3. We have checked our frequency calculations by determining the vibrational modes of CO adsorbed on the regular $TiO_2(110)$ rutile surface. Here, CO is bound to the Ti_{5c} cations and the frequency is blue-shifted by the interaction of the CO dipole with the electric field associated to the Ti^{4+} cation (first-order Stark effect). The experimental frequency, 2192−2209 cm^{-1},[55,56] is reproduced with sufficient accuracy, 2197 cm^{-1}, Table 3.

The computed C−O frequency of gas-phase AuCO, 2097 cm^{-1}, is red-shifted by 46 cm^{-1} with respect to free CO, Table 3. This is due to the back-donation of charge into the CO $2\pi^*$ levels. The frequency of CO adsorbed on a Au atom bound to an OT site is 2151 cm^{-1}, Table 3. This frequency is slightly higher than that of free CO, consistent with the fact that the Au atom carries a partial positive charge. Of course, the positive shift is mitigated by the back-donation of charge from the metal orbitals to the CO $2\pi^*$ levels, and the result is a very small shift, +8 cm^{-1}. A relatively high value of the CO frequency is consistent with the analyses presented above and provides further support of the occurrence of a charge transfer from Au to TiO_2 on regular sites induced by CO adsorption.

When AuCO is formed at an oxygen vacancy ($Au^{\delta-}$), the CO frequency is 2073 cm^{-1}, that is, 70 cm^{-1} smaller than in the gas phase. This is consistent with the presence of an increased electron density on Au. Therefore, going from Au_1 on a regular OT site to Au_1 on an oxygen vacancy, OV, there is a change in CO frequency of 78 cm^{-1}. This should be sufficient to detect the presence of differently bound complexes on the surface.

To summarize, the theoretical results for CO adsorbed on Au atoms deposited on regular or defect sites of the $TiO_2(110)$ rutile surface show two completely different situations: a strong Au−CO bond, 2.4 eV, a positive CO ω shift on OT sites (bridging oxygen rows of the oxidized TiO_2 surface), a weak Au−CO bond (0.4 eV), and a negative CO ω shift on OV sites (oxygen vacancies on reduced TiO_2).

Discussion

The IR spectra of the $Au^{13}CO$ complexes formed at the TiO_2 surface show three main bands. The first one, present up to 150 K, is observed at ~2140 cm^{-1} (~2190 cm^{-1} for ^{12}CO) and is due to CO adsorbed on five-coordinated Ti cations; see Table 3. This band corresponds to that at 2192 cm^{-1} for ^{12}CO reported in previous studies.[55,56] For temperatures higher than 150 K, CO desorbs from these sites and the band disappears, Figures 1 and 2. $Au^{13}CO$ complexes have been generated on reduced and oxidized surfaces in two ways. In the first case, gold atoms are deposited in a ^{13}CO background so that $Au^{13}CO$ complexes can form directly in the gas phase or upon deposition. On an oxidized surface, the $Au^{13}CO$ complexes will bind to regular sites; therefore, the intense band at ~2125 cm^{-1} (~2175 cm^{-1} for ^{12}CO) can be assigned to these species. The band is blue-shifted by about 30 cm^{-1} with respect to that of free ^{13}CO, 2093 cm^{-1}, Table 3, and is present up to 380 K, indicating a significant thermal stability of these species. Using a Redhead equation with a pre-exponential factor 10^{13}, this corresponds to a Au−CO binding energy of about 1 eV. On a reduced surface, the IR band at ~2125 cm^{-1} is accompanied by a low-frequency feature at ~2080 cm^{-1} (~2129 cm^{-1} for ^{12}CO) (Figure 2), moderately red-shifted with respect to free ^{13}CO, which can be attributed to $Au^{13}CO$ complexes formed in correspondence of point defects. This assignment is corroborated by another experiment where gold atoms are deposited first on the titania surface, and then exposed to ^{13}CO. In this case, the Au atoms can diffuse on the surface and become stabilized at the most strongly binding sites before they interact with ^{13}CO. Thus, the majority of $Au^{13}CO$ complexes should form in correspondence of surface defects. The low-temperature IR spectra show an intense band at ~2140 cm^{-1} due to ^{13}CO adsorbed on Ti sites (~2190 cm^{-1} for ^{12}CO), and a weaker band at ~2080 cm^{-1} likely due to $Au^{13}CO$ complexes formed at defect sites (~2129 cm^{-1} for ^{12}CO). Both of these bands disappear at 175 K, indicating desorption of ^{13}CO from Ti sites and from Au atoms bound to defects. This temperature corresponds to a $Au^{13}CO$ binding energy of about 0.4 eV.

To summarize, the experiments suggest that $Au^{13}CO$ complexes formed at regular sites are stable up to 380 K (Au−CO bond strength of about 1 eV) and have a ^{13}CO stretching at ~2120 cm^{-1}, blue-shifted with respect to free ^{13}CO. $Au^{13}CO$ complexes formed at defects are stable only up to 175 K (Au−CO bond strength of about 0.4 eV) and have a ^{13}CO frequency at ~2080 cm^{-1}, that is, red-shifted with respect to free ^{13}CO.

These results have now to be interpreted in view of the theoretical data. First of all, we have seen that Au atoms are able to diffuse freely on the $TiO_2(110)$ rutile surface for temperatures around 100 K (diffusion barrier of <0.2 eV). This confirms that Au atoms deposited on the surface before exposure to CO can migrate on the surface until they become trapped at existing defects, most likely oxygen vacancies which bind Au atoms very strongly, 1.7 eV (reduced films). Thus, for reduced samples, the large majority of the Au atoms is expected to occupy oxygen vacancy sites when CO is introduced in the chamber. CO then binds to Ti^{4+} sites with $D_e = 0.40$ eV and $\omega_e = 2197$ cm^{-1}; it binds also to Au atoms sitting on oxygen vacancies with the same energy, $D_e = 0.41$ eV, and $\omega_e = 2073$ cm^{-1}. This shows that (a) CO will desorb simultaneously from Ti^{4+} sites and from Au atoms bond at defects and (b) that

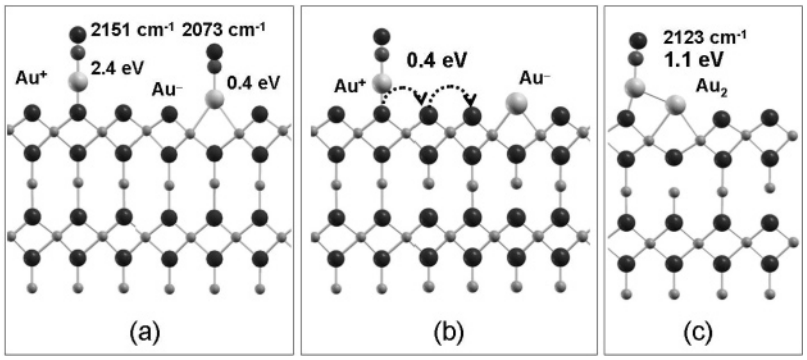

Figure 7. Schematic representation of the evolution of TiO_2Au_1CO as function of temperature increase (reduced TiO_2 surface). (a) Low-temperature (<150 K): AuCO complexes formed on bridging oxygens (OT sites) and on oxygen vacancies (OV sites) coexist. (b) Temperatures > 150 K: CO desorbs from Au atoms bound at oxygen vacancies, and AuCO complexes formed on regular sites start to diffuse. (c) Diffusing AuCO complexes bind to Au atoms stabilized at oxygen vacancies with formation of Au_2CO species. For T > 380 K, CO desorbs from these species.

the CO frequency for AuCO complexes formed at vacancies is considerably red-shifted with respect to free CO, Table 3. This is in qualitative agreement with the experimental measurements, thus providing a signature of the fact that a charge transfer has occurred from the surface to Au, which carries a partial negative charge. Still, we notice a quantitative discrepancy between the predicted CO frequency for AuCO formed on a vacancy, 2073 cm^{-1}, and the measured values scaled to ^{12}CO, ~2129 cm^{-1}.

When we consider AuCO complexes formed on bridging oxygen sites of the nondefective surface, the computed CO ω_e is 2151 cm^{-1}, that is, blue-shifted with respect to free CO, Table 3, and the Au−CO bond is very strong, 2.4 eV. This is due to the partial positive charge carried by the Au atom as a consequence of the charge transfer to TiO_2 induced by CO. The considerably higher frequency of AuCO complexes formed at regular sites (OT) as compared to oxygen vacancies (OV) observed experimentally, $\Delta\omega \approx 40$ cm^{-1}, is confirmed by the calculations where the shift is $\Delta\omega \approx 80$ cm^{-1}. These conclusions are fully consistent with the XPS analysis of CO adsorbed on Au_1/TiO_2 recently performed by Lee et al.[20] CO adsorbed on dispersed Au atoms interacting with regular sites results in a 1 eV shift in the Au 4f binding energy to higher energy, indicating that the atoms are in positive oxidation state, and in a substantial Au−CO bonding, while CO adsorbs weakly on Au-vacancy complexes.[20]

The computed Au−CO bond strength on OT sites, 2.4 eV, is more than 2 times that deduced experimentally (~1 eV) and should correspond to a AuCO complex stable up to about 800 K, in clear contradiction with the experiment. To rationalize this result, one has to consider diffusion processes occurring on the surface when the temperature is increased. This is schematically illustrated in Figure 7 for the case of a reduced TiO_2 surface. At very low temperature, below 100 K, AuCO complexes formed in the gas phase or upon deposition and bound to regular sites of the surface (bridging oxygens) are rather immobile as their diffusion barrier along the oxygen rows is estimated to be of about 0.4 eV. Because the AuCO bond on these sites is very strong, 2.4 eV, the complex becomes mobile before to release CO. Thus, as the temperature approaches 150 K, two phenomena occur: (1) CO molecules desorb from Au atoms bound at the oxygen vacancies and from Ti^{4+} sites ($D_e \approx 0.4$ eV in both cases); and (2) the AuCO complexes formed on the oxygen rows (regular sites) become mobile on the surface (diffusion barrier ~0.4 eV). Therefore, around 150−200 K, the Au atoms bound to oxygen vacancies (if present) lose their CO molecules, while AuCO complexes formed on oxygen rows begin to diffuse. In their diffusion path, the AuCO complexes have a high probability to become trapped at an empty oxygen vacancy, with immediate release of the CO molecule, or to bind to Au atoms stabilized at oxygen vacancies. When this occurs, they form Au_2CO complexes. The binding of CO to Au_2 bound at oxygen vacancies is 1.1 eV, that is, is consistent with a desorption temperature of 350−400 K. While this is not necessarily the only mechanism that leads to CO desorption around room temperature from reduced TiO_2 surfaces, it is indicative that the AuCO complexes formed on regular sites migrate on the surface until they further react to produce new species where CO is less strongly bound.

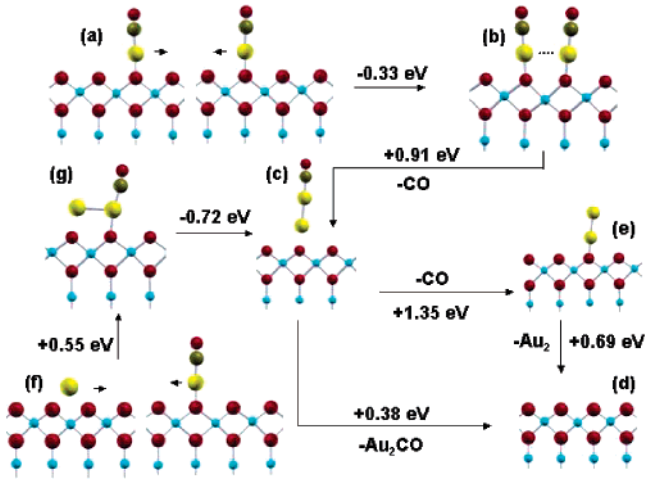

Figure 8. Schematic representation of the evolution of TiO_2Au_1CO as a function of temperature increase (oxidized TiO_2 surface). (a) AuCO complexes diffuse along bridging oxygens (OT sites). (b) Formation of a $(AuCO)_2$ dimer. (c) Release of a CO molecule and formation of Au_2CO. (d) Desorption of Au_2CO. (e) Desorption of a CO molecule from supported Au_2CO. (f) Interaction of a Au atom and of a AuCO complex diffusing along bridging oxygens (OT sites). (g) Formation of a metastable Au_2CO complex, which then evolves in the most stable isomer (c).

Figure 8 summarizes the case where the AuCO species diffuse on an oxidized TiO_2 surface (also in this case no CO is present above 380 K, Figure 1). Two diffusing AuCO units, Figure 8a, form a weakly bound $(AuCO)_2$ dimer where the Au−Au bond is quite long, 3.25 Å, Figure 8b. This is not surprising if we consider that formally the interacting species are $AuCO^+$ complexes. The $(AuCO)_2$ dimer releases one CO molecule with an energy cost of 0.91 eV, Figure 8c. This means that around room temperature two AuCO complexes colliding on the surface can reversibly form the $(AuCO)_2$ dimer and that, if there is enough thermal energy in the system, CO can desorb from the dimer before it breaks apart. When this occurs, one is left with

a Au_2CO complex that consists of a Au_2 molecule adsorbed with the molecular axis normal to the surface, Figure 8c, and the CO molecule on top of it (r(Au−Au) = 2.52 Å). The Au_2CO unit, however, is weakly bound to TiO_2 and can desorb with a cost of 0.38 eV, only leaving behind the clean TiO_2 surface, Figure 8d. It can also lose a second CO molecule, with formation of a Au_2 molecule adsorbed on TiO_2, but in this case the cost is 1.35 eV, Figure 8e (notice that at this point also the Au_2 molecule will desorb, because its adsorption energy is of 0.69 eV only, Figure 8d). Another possibility (less probable) is the interaction of a single Au atom with a AuCO complex, Figure 8f, with formation of a Au_2CO metastable intermediate, Figure 8g, which will then evolve into the most stable isomer shown in Figure 8c. The formation of Au_2CO from diffusing Au and AuCO species, Figure 8c, is weakly exothermic, by 0.17 eV. Once formed, this species will evolve as described above for elevated temperatures, that is, by desorbing the entire Au_2CO unit or smaller fragments. In conclusion, even on the oxidized TiO_2 surface, the aggregation of the stable AuCO complexes leads to dimeric species from which CO desorbs more easily than from the AuCO monomer. The calculations indicate that the key step is the release of a CO molecule from the $(AuCO)_2$ dimer, a process which costs about 0.9 eV. This energy is consistent with CO desorbing from the surface around room temperature.

Conclusions

We have studied the adsorption of Au atoms on TiO_2 thin films grown on Mo(110) and their interaction with adsorbed CO molecules. The combined use of IR spectra measured as a function of temperature and film preparation (oxidized or reduced films) and of DFT calculations allows us to draw some general conclusions.

(1) In agreement with most of previous studies,[5,8−10,18] the calculations show that gold atoms bind weakly on regular sites of the TiO_2(110) rutile surface (D_e < 0.5 eV). The atoms keep the $5d^{10}6s^1$-like atomic configuration, and little or no charge transfer occurs on these sites. Gold atoms diffusion occurs even at low temperature (diffusion barrier < 0.2 eV).

(2) Diffusing Au atoms can be trapped at oxygen vacancies[8−10] where they bind strongly to the substrate (computed D_e = 1.7 eV). On these sites, there is a charge transfer from the TiO_2 substrate to Au, which becomes formally Au^-.

(3) AuCO complexes formed on oxygen vacancies are characterized by a weak Au−CO bond (D_e = 0.4 eV) and by a red-shift in the CO ω_e. Both of these properties are a direct consequence of the excess of negative charge on the Au adatom.

(4) On bridging oxygen sites of the TiO_2 surface, CO induces a charge transfer from Au to TiO_2, with formation of a $Au^{\delta+}$ adatom. This leads to a very strong Au−CO bond (D_e = 2.4 eV) and to a blue-shift of the CO stretching frequency with respect to gas-phase CO.

(5) CO adsorption on TiO_2Au_1 has been used to distinguish between Au atoms bound on regular sites ($Au^{\delta+}$) or on oxygen vacancies ($Au^{\delta-}$). The results of IR measurements are fully consistent with this picture. On oxidized TiO_2 surfaces, the AuCO species formed are thermally stable up to 380 K and the CO frequency is blue-shifted with respect to free CO. On reduced surfaces, a weaker feature has been assigned to AuCO complexes formed on oxygen vacancies. These latter species are stable only up to 150 K and exhibit a red-shifted CO frequency.

(6) We have proposed some possible mechanisms to reconcile the observed CO desorption at 380 K with the unusually high stability of Au−CO complexes formed on regular sites predicted by the calculations. This is connected with the diffusion of AuCO complexes along the bridging rows of the rutile surface for temperatures above 150 K; this finally leads to the formation of gold dimers when the diffusing AuCO complex encounters an Au atom occupying an oxygen vacancy (reduced TiO_2) or a second AuCO unit (oxidized TiO_2). The resulting dimer complex binds CO by about 1 eV, consistent with a thermal stability up to 350−400 K.

Acknowledgment. This work has been supported by the Italian MIUR through a Cofin 2003 project, the Deutsche Forschungsgemeinschaft, DFG, and the European Project STRP GSOMEN.

Supporting Information Available: Complete ref 41. This material is available free of charge via the Internet at http://pubs.acs.org.

References and Notes

(1) Chen, M. S.; Goodman, D. W. *Science* **1998**, *281*, 1647.
(2) Valden, M.; Lai, X.; Goodman, D. W. *Science* **2004**, *306*, 252.
(3) Diebold, U. *Surf. Sci. Rep.* **2003**, *48*, 53.
(4) Sorescu, D. C.; Yates, J. T. *J. Phys. Chem. B* **2002**, *106*, 6184.
(5) Giordano, L.; Pacchioni, G.; Bredow, T.; Sanz, J. F. *Surf. Sci.* **2001**, *471*, 21.
(6) Lopez, N.; Norskov, J. K.; Janssens, T. V. W.; Carlsson, A.; Puig-Molina, A.; Clausen, B. S.; Grunwaldt, J. D. *J. Catal.* **2004**, *225*, 86.
(7) Xu, C.; Oh, W. S.; Liu, G.; Kim, D. Y., Goodman, D. W. *J. Vac. Sci. Technol., A* **1997**, *15*, 1261.
(8) Okazaki, K.; Morikawa, Y.; Tanaka, S.; Tanaka, K.; Kohyama, M. *Phys. Rev. B* **2004**, *69*, 235404.
(9) Wang, Y.; Hwang, G. S. *Surf. Sci.* **2003**, *542*, 72.
(10) Vijay, A.; Mills, G.; Metiu, H. *J. Chem. Phys.* **2003**, *118*, 6536.
(11) Minato, T.; Susaki, T.; Shiraki, S.; Kato, H. S.; Kawai, M.; Aika, K. I. *Surf. Sci.* **2004**, 566−568, 1012.
(12) Wahlstrom, E.; Lopez, N.; Schaub, R.; Thostrup, P.; Ronnau, A.; Africh, C.; Laegsgaard, E.; Norskov, J. K.; Besenbacher, F. *Phys. Rev. Lett.* **2003**, *90*, 026101.
(13) Meier, D. C.; Goodman, D. W. *J. Am. Chem. Soc.* **2004**, *126*, 1892.
(14) Lee, S. S.; Fan, C. Y.; Wu, T. P.; Anderson, S. L. *J. Am. Chem. Soc.* **2004**, *126*, 5682.
(15) Molina, L. M.; Rasmussen, M. D.; Hammer, B. *J. Chem. Phys.* **2004**, *120*, 7673.
(16) Boccuzzi, F.; Chiorino, A.; Manzoli, M. *Surf. Sci.* **2000**, *454−456*, 942.
(17) Boccuzzi, F.; Chiorino, A.; Manzoli, M. *Surf. Sci.* **2002**, *502−503*, 513.
(18) Manzoli, M.; Chiorino, A.; Boccuzzi, F. *Surf. Sci.* **2003**, *532−535*, 377.
(19) Vittadini, A.; Selloni, A. *J. Chem. Phys.* **2002**, *117*, 353.
(20) Lee, S.; Fan, C.; Wu, T.; Anderson, S. L. *Surf. Sci.* **2005**, *578*, 5.
(21) Arrii, S.; Morfin, F.; Renouprez, A. J.; Rousset, J. L. *J. Am. Chem. Soc.* **2004**, *126*, 1199.
(22) Haruta, M. *Catal. Today* **1997**, *36*, 153.
(23) Cosandey, F.; Madey, T. E. *Surf. Rev. Lett.* **2001**, *8*, 73.
(24) Socaciu, L. D.; Hagen, J.; Bernhardt, T. M.; Wöste, L.; Heiz, U.; Häkkinen, H.; Landman, U. *J. Am. Chem. Soc.* **2003**, *125*, 10437.
(25) Yoon, B.; Häkkinen, H.; Landman, U.; Wörz, A. S.; Antonietti, J.-M.; Abbet, S.; Heiz, U. *Science* **2005**, *307*, 403.
(26) Yan, Z.; Chinta, S.; Mohamed, A. A.; Fackler, J. P.; Goodman, D. W. *J. Am. Chem. Soc.* **2005**, *127*, 1604.
(27) Abbet, S.; Sanchez, A.; Heiz, U.; Schneider, W.-D.; Ferrari, A. M.; Pacchioni, G.; Rösch, N. *J. Am. Chem. Soc.* **2000**, *122*, 3453.
(28) Abbet, S.; Riedo, E.; Brune, H.; Heiz, U.; Ferrari, A. M.; Giordano, L.; Pacchioni, G. *J. Am. Chem. Soc.* **2001**, *123*, 6172.
(29) Oh, W. S.; Xu, C.; Kim, Y. D.; Goodman, D. W. *J. Vac. Sci. Technol., A* **1997**, *15*, 1710.
(30) Guo, Q.; Oh, W. S.; Goodman, D. W. *Surf. Sci.* **1999**, *437*, 49.
(31) Lai, X.; Guo, Q.; Min, B. K.; Goodman, D. W. *Surf. Sci.* **2001**, *487*, 1.
(32) Göpel, W.; Rocker, G.; Feierabend, R. *Phys. Rev. B* **1983**, *28*, 3427.
(33) Pan, J.-M.; Maschhoff, B. L.; Diebold, U.; Madey, T. E. *J. Vac. Sci. Technol., A* **1992**, *10*, 2470.
(34) Lu, G.; Linsebigler, A.; Yates, J. T. J. *J. Phys. Chem. B* **1994**, *98*, 11733.

(35) Diebold, U.; Anderson, J. F.; Ng, K.-O.; Vanderbilt, D. *Phys. Rev. Lett.* **1996**, *77*, 1322.
(36) Diebold, U.; Lehman, J.; Mahmoud, T.; Kuhn, M.; Leonardelli, G.; Hebenstreit, W.; Schmid, M.; Varga, P. *Surf. Sci.* **1998**, *411*, 137.
(37) Wang, L.-Q.; Baer, D. R.; Engelhard, M. H. *Surf. Sci.* **1994**, *320*, 306.
(38) Heiz, U.; Vanolli, F.; Trento, L.; Schneider, W.-D. *Rev. Sci. Instrum.* **1997**, *68*, 1986.
(39) Perdew, J. P.; Chevary, J. A.; Vosko, S. H.; Jackson, K. A.; Pederson, M. R.; Singh, D. J.; Fiolhais, C. *Phys. Rev. B* **1992**, *46*, 6671.
(40) Kresse, G.; Hafner, J. *Phys. Rev. B* **1993**, *47*, R558.
(41) Kresse, G.; Furthmüller, J. *Phys. Rev. B* **1996**, *54*, 11169.
(42) Vanderbilt, D. *Phys. Rev. B* **1990**, *41*, R7892.
(43) Onishi, H.; Aruga, T.; Egawa, C.; Iwasawa, Y. *Surf. Sci.* **1988**, *199*, 597.
(44) Rasmussen, M. D.; Molina, L. M.; Hammer, B. *J. Chem. Phys.* **2004**, *120*, 988.
(45) Wu, X.; Selloni, A.; Nayak, S. K. *J. Chem. Phys.* **2004**, *120*, 4512.
(46) Bates, S. P.; Kresse, G.; Gillan, M. J. *Surf. Sci.* **1997**, *385*, 386.
(47) Bredow, T.; Giordano, L.; Cinquini, F.; Pacchioni, G. *Phys. Rev. B* **2004**, *70*, 035419.
(48) Harris, L. A.; Quong, A. A. *Phys. Rev. Lett.* **2004**, *93*, 086105.
(49) Bredow, T.; Pacchioni, G. *Chem. Phys. Lett.* **2002**, *355*, 417.
(50) *CRC Handbook of Chemistry and Physics*, 74th ed.; Weast, R. C., Ed.; CRC Press: Cleveland, OH, 1994.
(51) The calculations have been done with the Gaussian03 code (Frisch, M. J.; et al. *Gaussian 03*, revision A.1; Gaussian, Inc.: Pittsburgh, PA, 2003) using Gaussian-type basis functions and the PW91 exchange-correlation functional.
(52) Judai, K.; Abbet, S.; Wörz, A. S.; Heiz, U.; Giordano, L.; Pacchioni, G. *J. Phys. Chem. B* **2003**, *107*, 9377.
(53) Linsebigler, A.; Lu, G.; Yates, J. T. *J. Chem. Phys.* **1995**, *103*, 9438.
(54) Neumaier, M.; Weigend, F.; Hampe, O.; Kappes, M. M. *J. Chem. Phys.* **2005**, *122*, 104702.
(55) Hadjiivanov, K.; Lamotte, J.; Lavalley, J.-C. *Langmuir* **1997**, *13*, 3374.
(56) Liao, L.-F.; Lien, C.-F.; Shieh, D.-L.; Chen, M.-T.; Lin, J.-L. *J. Phys. Chem. B* **2002**, *106*, 11240.